UNIVERSITY OF
LEADING
THE WAY
WESTMINSTER⌗

WestminsterResearch

http://www.westminster.ac.uk/research/westminsterresearch

3D Reconstruction of Medical Images from Slices Automatically Landmarked with Growing Neural Models

Anastassia Angelopoulou[1]
Alexandra Psarrou[1]
Jose Garcia-Rodriguez[2]
Sergio Orts-Escolano[2]
Jorge Azorin-Lopez[2]
Kenneth Revett[3]

[1]Faculty of Science and Technology, University of Westminster, UK
[2]Department of Computing Technology, University of Alicante, Spain
[3]Faculty of Informatics and Computer Science, British University in Egypt, Egypt

$3D$ Reconstruction of Medical Images from Slices Automatically Landmarked with Growing Neural Models

Anastassia Angelopoulou, Alexandra Psarrou

Faculty of Science and Technology, University of Westminster, Cavendish, W1W 6UW, United Kingdom.

Jose Garcia-Rodriguez, Sergio Orts-Escolano, Jorge Azorin-Lopez

Department of Computing Technology at University of Alicante. Po Box 99, 03080, Alicante, Spain

Kenneth Revett

British University in Egypt, Faculty of Informatics and Computer Science, ElSherouk City, Egypt.

Abstract

In this study, we utilise a novel approach to segment out the ventricular system in a series of high resolution T1-weighted MR images. We present a brain ventricles fast reconstruction method. The method is based on the processing of brain sections and establishing a fixed number of landmarks onto those sections to reconstruct the ventricles 3D surface. Automated landmark extraction is accomplished through the use of the self-organising network, the Growing Neural Gas (GNG), which is able to topographically map the low dimensionality of the network to the high dimensionality of the contour manifold without requiring a priori knowledge

Email addresses: `agelopa@wmin.ac.uk` (Anastassia Angelopoulou),
`psarroa@wmin.ac.uk` (Alexandra Psarrou), `jgarcia@dtic.ua.es` (Jose
Garcia-Rodriguez), `sorts@dtic.ua.es` (Sergio Orts-Escolano), `jazorin@dtic.ua.es`
(Jorge Azorin-Lopez), `ken.revett@bue.edu.eg` (Kenneth Revett)

of the input space structure. Moreover, our GNG landmark method is tolerant to noise and eliminates outliers. Our method accelerates the classical surface reconstruction and filtering processes. The proposed method offers higher accuracy compared with methods with similar efficiency as Voxel Grid.

1. Introduction

The cerebral ventricles are buried within the centre of the brain parenchyma and are the source of cerebral spinal fluid, which provides nutritive and cushioning support to the brain and spinal cord. Neuropathologies involving the ventricles range from severe hypertrophy diagnostic for hydrocephalus, to mild and diffuse enlargements associated with AIDS, Alzheimer's Disease and Schizophrenia [14, 19]. Currently, MRI techniques are employed routinely in the diagnosis of ventricular related diseases. In many cases, the extent of disease progression can be determined by quantifying the extent of the change in ventricular morphology and/or volume [14]. The usual practise in a clinical setting is to perform a high resolution T1-weighted MRI followed by laborious post-processing steps. The first stage in the post-processing step is to segment out the ventricles, which can be difficult in many cases if the patient is not properly aligned in the scanner. Next, the ventricles must be segmented followed by volumetric quantification. These post-processing steps are laborious and must be very accurate if the purpose of the scan is to help determine the extent of disease progression. In very overburdened medical facilities, performing this task manually may not be feasible. In addition, in a multi-centre study or when a patient visits multiple medical facilities, there is little assurance that the post-processing steps will be performed in an identical fashion. An automated procedure may provide the means of yielding

2

objective and consistent results across various institutions. It is imperative therefore that an accurate, rapid and automated algorithm be developed and deployed. That is the subject of the rest of this paper.

In this work, we introduce a new and computationally inexpensive method for the automatic selection of landmarks along the contours of $2D$ MRI slices of human brain. The incremental neural network, the growing neural gas (GNG) is used to automatically annotate the training set without using *a priori* knowledge of the structure of the input patterns. Unlike other methods, the incremental character of the model avoids the necessity to previously specify a reference shape. The method is used for the representation of two-dimensional outline of the ventricles, which is extended to the representation in three dimensions. As will be discussed in Section 3, GNG does not use any *a priori* knowledge, as its adaptation process is incremental based on competitive hebbian learning. To evaluate the accuracy of the method we have tested it with other self-organising models such as Kohonen maps and Neural Gas (NG) maps and global distance error has been applied to measure the quality of the adaptation of the network. We also obtained a 3D volume reconstruction of landmarked ventricles and compared our results with other reconstructions methods.

The remaining of the paper is organised as follows. In Section 2 a review of most used $2D$ and $3D$ methods is presented. Section 3 describes the topology learning including an introduction of statistical shape models and its application to automated ventricular segmentation, GNG learning algorithm and the error measurement used for the adaptation process. A set of experimental results is presented in Section 4 that includes 2D and 3D respresentations and comparative studies, followed by our major conclusions and future work.

3

2. Related Work

There are several algorithms that have been employed to perform automatic segmentation. These algorithms can be broadly classified into landmark and non-landmark based approaches. Non-landmark based techniques have been published using region-growing algorithms [41], level set [4], and rough sets based [46] techniques have been applied in the medical imaging domain.

Landmark based techniques can be classified as manual, semi-automatic and automatic. Because the first two are laborious and subjective especially when applied to $3D$ images, various attempts have been made to automate the process of landmark based image registration and correct correspondences among a set of shapes. Sousa's *et al.* [43] method uses the landmarks of the mean shape of an MRI foot data set as a reference to automatically generate the landmarks to the training set. The distance between the given landmark point from the mean shape and the nearest strong edge in the image is locally search. However,the method is arbitrary since the mean shape can be defined only for closed boundaries and for set of images that are mainly aligned and have small variations.

Davies *et al.* [11] presents a method to automatically build statistical shape models by re-paremeterising each shape from the training set and optimising an information theoretic function to assess the quality of the model has received a lot of attention recently. The quality of the model is assessed by adopting a minimum description length (MDL) criterion to the training set. This is a very promising method and the models that are produced are comparable to and often better than the manual built models. However, due to very large number of function evalua-tions and nonlinear optimisation the method is computationally expensive.

Fatemizadeh *et al.* [16] have used modified growing neural gas to automati-

cally correspond important landmark points from two related shapes by adding a third dimension to the data points and by treating the problem of correspondence as a cluster-seeking method by adjusting the centers of points from the two corresponding shapes. This is a promising method and has been tested to both synthetic and real data, but the method has not been tested on a large scale for stability and accuracy of building statistical shape models.

Three-dimensional reconstruction of medical images (tissue sections, CT and autoradiographic slices) is now an integral part of biomedical research. Reconstruction of such data sets into 3D volumes, via the registrations of 2D sections, has gained an increasing interest. The registration of multiple slices is of outmost importance for the correct 3D visualization and morphometric analysis (e.g. surface and volume representation) of the structures of interest. Several alignment algorithms have been proposed in that framework. Some interesting reviews of general medical image registration methods are presented in [6, 47, 30, 22]. The principal 3D alignment (reconstruction from 2D images) methods may be classified in the following categories: fiducial marker-based methods [21], feature based methods using contours, crest lines or characteristic points extracted from the images [28, 39], and gray level-based registration techniques using the intensities of the whole image [27, 2, 24, 38]. Most of the above mentioned techniques do not simultaneously consider the two major difficulties involved in medical and CT scanned data registration. At first, consecutive slices may differ significantly due to distortions, discontinuities in anatomical structures, cuts and tears. These effects are more pronounced when distant slices are involved in the registration. From this point of view, a registration method must be robust to missing data or outliers [27, 38]. Besides, registering the slices sequentially (the second with re-

spect to the first, the third with respect to the second, etc.) leads to different types of misregistration. If an error occurs in the registration of a slice with respect to the preceding slice, this error will propagate through the whole volume .Also, if the number of slices to be registered is large, a global offset of the volume may be observed, due to error accumulation [2]. In [27] is described a fully-automated algorithm for the alignment of 2D serially acquired sections forming a 3D volume. The approach relies on the optimization of a global energy function, based on the object shape, measuring the similarity between a slice and its neighborhood in the 3D volume. Slice similarity is computed using the distance transform measure in both directions. Osechinskiy and Kruggel [37] presents a flexible framework for intensity-based slice to volume nonrigid registration algorithms with a geometric transformation deformation field parameterized by various classes of spline functions. Algorithms are applied to cross-modality registration of histological and magnetic resonance images of the human brain. In [10] is presented a protocol that matches a series of stained histological slices of a baboon brain with an anatomical MRI scan of the same subject using an intermediate 3D-consistent volume of blockface photographs taken during the sectioning process. While [46] presents an automated multi-spectral MRI segmentation technique based on approximate reducts derived from the data mining paradigm.

2.1. 3D Reconstruction Methods

This section will review the most used methods and techniques for the reconstruction of generic three-dimensional surfaces.

2.1.1. Delaunay and $alpha$-shapes

Reconstruction with Delaunay methods in three dimensions consists of the extraction of tetrahedron surfaces from the initial point cloud. The concept of alpha-shape formalizes the intuitive notion of "shape" for a set of points in the space. One of the earliest approaches is based on -shapes of Edelsbrunner and Mucke [15]. Given a finite point set S, and the real parameter $alpha$, the $alpha$-shape of S is a polytope (the generalization to any dimension of a two dimensional polygon and a three-dimensional polyhedron) which is neither convex nor necessarily connected. For a large value, the $alpha$-shape is identical to the convex-hull of S. If the alpha value decreases progressively non-convex shapes with cavities are obtained. The algorithm proposed by Edelsbrunner and Mucke, eliminates all tetrahedrons which are delimited by a surrounding sphere smaller than . The surface is then obtained with the external triangles from the resulting tetrahedron. Another approach is based on labeling the initial tetrahedrons as interior and exterior. The resulting surface is generated from the triangles found in and out. This idea first appeared in [5] and was later performed by Powercrust in [1] and the algorithm called Tight Cocone [12]. Both methods have been recently extended for reconstructing point clouds with noise [13, 34]. The main advantage of most Delaunay based methods is that fit very accurately the surface defined by the original point cloud. However, the method is very sensitive to noise since it is and interpolation based method producing undesirable results with noisy data. Therefore, the quality of the points obtained in the digitization process determines the feasibility of these methods. Due to the use of the whole point cloud set to obtain the most accurate triangulation, considering the Delaunay rule, the digitized points on the surface with an error considered above the limit, will be explicitly

7

represented on the reconstructed surface geometry. Moreover, the application of any of these techniques requires the computation of the normal orientation, which is unfeasible from the point of view of efficiency of the model, since the time needed for the shoe last geometry reconstruction by these techniques exceed the limits established in the context of the problem.

2.1.2. Zero Set Methods

Implicit reconstruction methods (or zero-set methods) reconstruct the surface using a distance function which assigns to each point in the space a signed distance to the surface S. The polygonal representation of the object is obtained by extracting a zero-set using a contour algorithm. Thus, the problem of reconstructing a surface from a disorganized point cloud is reduced to the definition of the appropriate function f with a zero value for the sampled points and different to zero value for the rest. Lorensen et al. [29] established the use of such methods with the algorithm called Marching-Cubes. This algorithm has evolved in different variants, [23] used a discrete function f, in [7] a polyharmonic radial basis function is use to adjust the initial point set. Other approaches include the adjustment function Moving Least Squares [42, 17] and basic functions with local support [44], based on the Poisson equation [35]. Those methods have the problem of loss of the geometry precision in areas with extreme curvature, i.e., corners, edges. Furthermore, pretreatment of information by applying some kind of filtering technique also affects the definition of the corners, soften them. There are several studies related to post-processing techniques used in the reconstruction for the detection and refinement of corners [17, 45] but these methods increase the complexity of the solution.

2.1.3. Voxel Grid

The Voxel Grid filtering technique is based on the input space sampling using a grid of 3D voxels to reduce the number of points. This technique has been used traditionally in the area of computer graphics to subdivide the input space and reduce the number of points [8, 25]. For each voxel, a centroid is chosen as the representative of all points. There are two approaches, the selection of the voxel centroid or select the centroid of the points lying within the voxel. To obtain internal points average has a higher computational cost, but offers better results. Thus, a subset of the input space is obtained that roughly represents the underlying surface. The Voxel Grid method presents the same problems as other filtering techniques: impossibility of defining the final number of points that represent the surface, geometric information loss due to the reduction of the points inside a voxel and sensitivity to noisy input spaces. This method will be compared with our GNG landmark based 3D reconstruction, as it offers similar features for efficient mesh reconstruction.

3. Topology Learning

One way of selecting points of interest along the contour of $2D$ shapes is to use a topographic mapping where a low dimensional map is fitted to the high dimensional manifold of the contour, whilst preserving the topographic structure of the data. A common way to achieve this is by using self-organising neural networks where input patterns are projected onto a network of neural units such that similar patterns are projected onto units adjacent in the network and vice versa. As a result of this mapping a representation of the input patterns is achieved that in postprocessing stages allows one to exploit the similarity relations of the in-

put patterns. Such models have been successfully used in applications such as speech processing [26], robotics [40, 32] and image processing [36]. However, most common approaches are not able to provide good neighborhood and topology preservation if the logical structure of the input patten is not known *a priori*. In fact, the most common approaches specify in advance the number of neurons in the network and a graph that represents topological relationships between them, for example, a two-dimensional grid, and seek the best match to the given input pattern manifold. When this is not the case the networks fail to provide good topology preserving as for example in the case of Kohonen's algorithm.

The approach presented in this paper is based on self-organising networks trained using the Growing Neural Gas learning method [18]. This is an incremental training algorithm where the number of units in the network are determined by the unifying measure for neighborhood preservation [20], the topographic product. The links between the units in the network are established through competitive hebbian learning [31]. As a result the algorithm can be used in cases where the topological structure of the input pattern is not known *a priori* and yields topology preserving maps of feature manifold [33].

3.1. Statistical Shape Models

When analysing biological shapes it is convenient and usually effective to describe them using statistical shape models. The most well known statistical shape models are Cootes *et al.* [9] 'Point Distribution Models' (PDMs) that models the shape of an object and its variation by using a set of n_p landmark points from a training set of S_i shapes. In this work, PDM represents the ventricles as a set of n_p automatically extracted landmarks (in our case 64, 100, 144 and 169 neurons) in a vector $\mathbf{x} = [x_{i_0}] \; \mathbf{x} = [x_{i_0}, x_{i_1}, ..., x_{in_{p-1}}, y_{i_0}, y_{i_1}, ..., y_{in_{p-1}}]^T$. In order to gen-

erate flexible shape models the S_i shapes are aligned (translated, rotated, scaled) and normalised (removing the centre-of-gravity and placing it at the origin) to a common set of axes. The modes of variations of the ventricles are captured by applying principal component analysis (PCA). The ith shape in the training set can be back-projected to the input space by a linear model of the form:

$$\mathbf{x} = \bar{\mathbf{x}} + \Phi\beta_i \tag{1}$$

where $\bar{\mathbf{x}}$ is the mean shape, Φ describes a set of orthogonal modes of shape variations, and β_i is a vector of weights for the ith shape. To ensure that the above weight changes describe reasonable variations we restrict the weight β_i to the range $-2\sqrt{\lambda} \leq \beta_i \leq 2\sqrt{\lambda}$ and the shape is back-projected to the input space using Equation (1). PCA works well as long as good correspondences exist. To obtain the correspondences and represent the contour of the ventricles a self-organising network GNG was used.

3.2. Growing neural gas

With Growing Neural Gas (GNG) [18] a growth process takes place from minimal network size and new units are inserted successively using a particular type of vector quantisation [26]. To determine where to insert new units, local error measures are gathered during the adaptation process and each new unit is inserted near the unit which has the highest accumulated error. At each adaptation step a connection between the winner and the second-nearest unit is created as dictated by the competitive hebbian learning algorithm. This is continued until an ending condition is fulfilled, as for example evaluation of the optimal network topology based on the topographic product [20]. This measure is used to detect deviations between the dimensionalities of the network and that of the input space,

11

detecting folds in the network and, indicating that is trying to approximate to an input manifold with different dimensions. In addition, in GNG networks learning parameters are constant in time, in contrast to other methods whose learning is based on decaying parameters.

In the remaining of this Section we describe the growing neural gas algorithm and ending condition as used in this work. The network is specified as:

- A set N of nodes (neurons). Each neuron $c \in N$ has its associated reference vector $w_c \in R^d$. The reference vectors can be regarded as positions in the input space of their corresponding neurons.

- A set of edges (connections) between pairs of neurons. These connections are not weighted and its purpose is to define the topological structure. An *edge aging scheme* is used to remove connections that are invalid due to the motion of the neuron during the adaptation process.

The GNG learning algorithm to map the network to the input manifold is as follows:

1. Start with two neurons a and b at random positions w_a and w_b in R^d.

2. Generate at random an input pattern ξ according to the data distribution $P(\xi)$ of each input pattern. In our case since the input space is $1D$, the input pattern is the (x, y) coordinate of the edges. Typically, for the training of the network we generated 1000 to 10000 input patterns depending on the complexity of the input space.

3. Find the nearest neuron (winner neuron) s_1 and the second nearest s_2.

4. Increase the age of all the edges emanating from s_1.

5. Add the squared distance between the input signal and the winner neuron to a counter error of s_1 such as:

$$\Delta error(s_1) = \|w_{s_1} - \xi\|^2 \tag{2}$$

6. Move the winner neuron s_1 and its topological neighbours (neurons connected to s_1) towards ξ by a learning step ϵ_w and ϵ_n, respectively, of the total distance:

$$\Delta w_{s_1} = \epsilon_w(\xi - w_{s_1}) \tag{3}$$

$$\Delta w_{s_n} = \epsilon_w(\xi - w_{s_n}) \tag{4}$$

for all direct neighbours n of s_1.

7. If s_1 and s_2 are connected by an edge, set the age of this edge to 0. If it does not exist, create it.

8. Remove the edges larger than a_{max}. If this results in isolated neurons (without emanating edges), remove them as well.

9. Every certain number λ of input patterns generated, insert a new neuron as follows:

- Determine the neuron q with the maximum accumulated error.

- Insert a new neuron r between q and its further neighbour f:

$$w_r = 0.5(w_q + w_f) \tag{5}$$

- Insert new edges connecting the neuron r with neurons q and f, removing the old edge between q and f.

10. Decrease the error variables of neurons q and f multiplying them with a consistent α. Initialize the error variable of r with the new value of the error variable of q and f.

11. Decrease all error variables by multiplying them with a constant γ.

12. If the stopping criterion is not yet achieved (in our case the stopping criterion is the number of neurons), go to step 2.

Our method is able to find a fixed number of landmarks placing them in an accurate way. The method is tolerant to noise and automatically delete outliers by using edge length average and reorder landmarks by using the own neural network neighborhood structure. The landmarks obtained for each of the acquired section serve automatically for building a tensor that represents the 3D surface.

The algorithm was tested with different number of neurons so that the best topological map can be achieved. The testing involved two cases were the number of neurons were too few or too excessive for the training set of the images. In the former the topological map is lost, not enough neurons to represent the contour of the ventricles and in the later an overfit is performed.

3.3. Error Minimisation

The goal of training a network is to minimise the expected *quantisation or distortion error*. In our case is to find the values of the reference vectors $w_c, c \in R^d$ of the input pattern distribution $P(\xi)$ such that the error:

$$E = \sum_{\forall \xi \in R^d} \| w_{s_\xi - \xi} \|^2 P(\xi) \tag{6}$$

14

is minimised, where s_ξ is the nearest neuron to the input pattern ξ.

In previous works [3], it was demonstrated that the distortion error for Kohonen maps is very big compared to NG and GNG but for NG the results are slightly better to GNG, since it has less distortion error thus better topology preservation, but the learning time is 20 times higher compared to GNG. However, as the number of neurons increases the distortion error decreases and stabilises for both networks. For both Kohonen and NG in the adaptation rule it is assumed that the numbers of weights are known and are not allowed to change. GNG overcomes this as it is a growth mechanism and new neurons are inserted based on local error measurements. Thus GNG can give better preservation compared to the other two and when tested to a larger scale of data set.

4. Experiments

The data that we used in this study was obtained from the MNI BIC Centre for Imaging at McGill University, Canada. These images are 1 mm thick, 181x217 pixels per slice ($1.0mm^2$ in-plane resolution), 3% noise and 20% INU. These images are used as our gold standard for segmentation, as every voxel in the entire volume has been correctly labelled to a tissue class by the McGill Institute. The entire brain volume consisted of 181 slices, from which we extracted those that contained ventricles (slices 49-91). The images are 16 bit grey scale, which were thresholded out manually to remove all but the outline of the ventricles. Since most typical clinical MRI volumes are on average 5 mm thick, we selected 4 groups of 5 contiguous slices to produce our point distribution model. Several experiments have been carried out to demonstrate the validity of our proposal. Different versions of the used methods have been developed and tested on

a desktop machine with an Intel Core i3 540 3.07Ghz. All these methods have been coded in C ++.

4.1. Variability and Comparison with Other Neural Networks

Figure 1 shows the modes of variation for all four groups are displayed by varying the first shape parameter $\beta_i\{\pm 2\sigma\}$ over the training set. The qualitatively results show that GNG leads to correct extraction of corners of anatomical shapes and are compact when the topology preservation of the network is achieved (Figure 3).
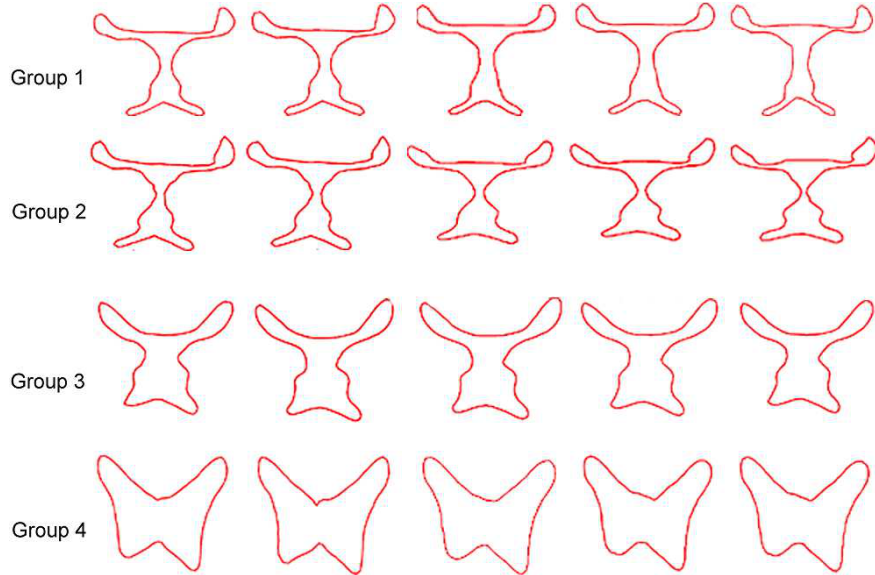
Figure 1: The first mode ($m = 1$) of variation for the four groups of 5 contiguous slices taken from MR brain data. Range of variation $-2\sqrt{\lambda} \leq \beta_i \leq 2\sqrt{\lambda}$.

In Figure 2 two shape variations from the automatically generated landmarks were superimposed to groups 4 and 3 from the training set. These modes effectively capture the variability of the training set and present only valid shape instances.

16

Figure 2: Superimposed shape instances to groups 4 and 3 from the training set.

Table 1 shows the total variance achieved by maps containing varying number of neurons (64, 100, 144, 169) used for the automatic annotation (Figure 3). The map of 100 neurons is the most compact since it achieves the least variance compared to 64, 144 and 169 neurons among the four groups. It is interesting to note that whilst there is significant difference between 64, and 169 neurons -not enough neurons to represent the object (Image A) and too many neurons (Image D)- the mapping with 100 is good and has no significant difference with the mapping of 144 neurons. The reason is that for the current size of the images the distance between the neurons is short enough so adding extra neurons does not give more accuracy in placement. Figure 4 shows superimposed the mean shapes of each group and for all neurons. The red shape referring to the 100 neurons is the most compact mean shape. We have tested and compared our method with two other SOMs, the Kohonen map and the NG map. The quantitative results show that GNG is significantly faster compared to Kohonen and NG, and the learning time
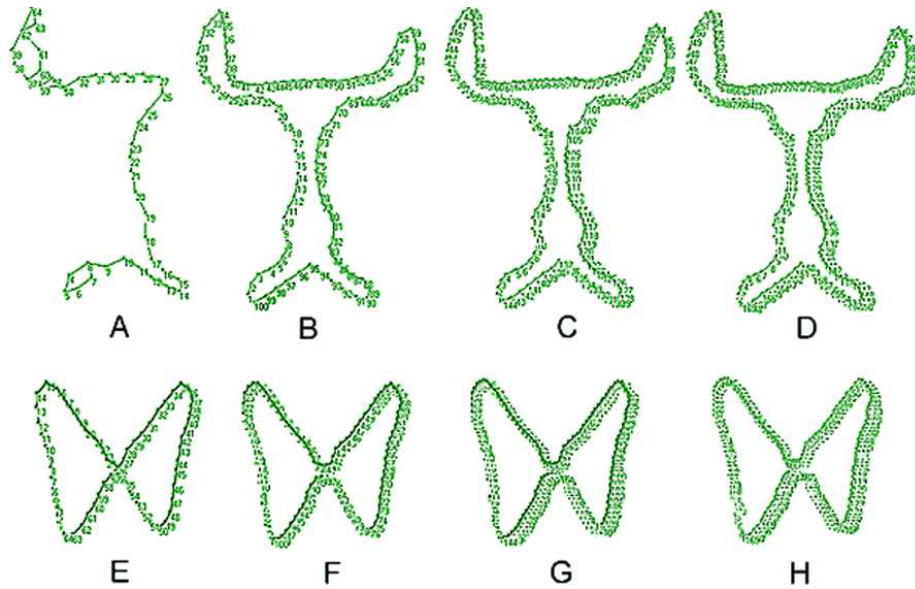
17

Figure 3: Automatic annotation with network size of 64 (Image A, E), 100 (Image B, F), 144 (Image C, G) and 164 (Image D, H) neurons for two groups of the MRI volumes of the ventricles.

is not so significant in GNG with the insertion of neurons compared to the other two where the adaptation process slows dramatically as the number of neurons increases.

Figure 5 shows a comparative diagram of the learning time of various SOMs and at different number of neurons. The adaptation with 64 neurons is only 3 sec with GNG compared to the 57 sec and 52 sec with Kohonen and NG, but with 64 neurons the topology preservation in most of the shapes is lost independent of the selection of the SOM. A good adaptation with 100 and 144 neurons takes 6 and 11 seconds respectively at 1000 patterns to adapt to the contour of the ventricles.

4.2. Voxel vs GNG comparison

Results have been compared with Voxel Grid method. Different parameters for GNG have been tested and compared using quality measures. Voxel Grid method

Groups	64 (neurons)	100 (neurons)	144 (neurons)	169 (neurons)
V_{T_1}	9.8340	1.9385	3.9668	3.9235
V_{T_2}	13.1873	1.7284	4.3672	3.1617
V_{T_3}	6.7822	2.0109	3.2260	4.0057
V_{T_4}	2.2567	1.6198	2.8398	3.5861

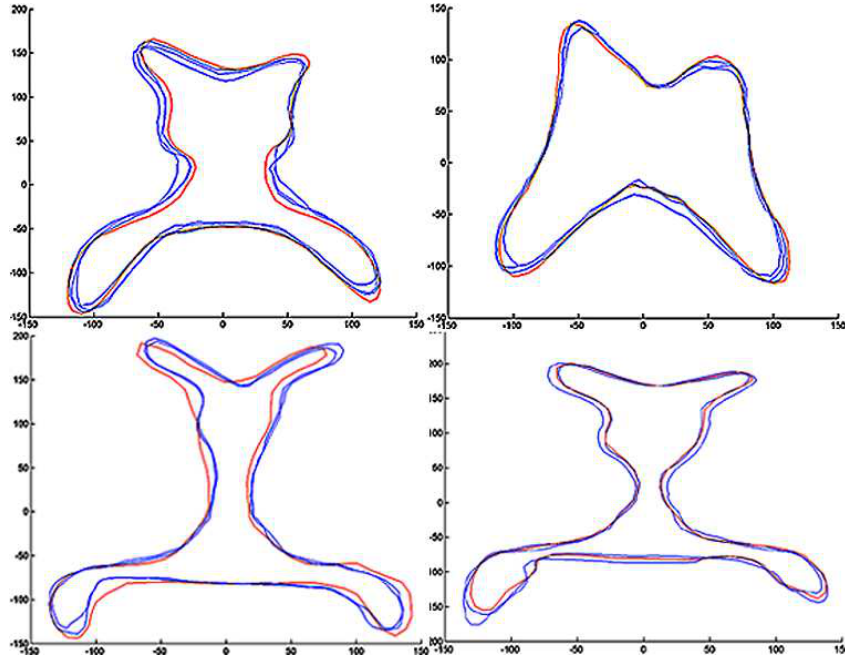Table 1: A quantitative comparison of various neurons adapted to the ventricle model with total variance per group.

Figure 4: The means of the four groups and for different neurons. The blue outlines represent the means of the 64, 144 and 169 neurons. The red outline represents the most compact mean achieved with the mapping of 100 neurons.

and visualization have been done using the PCL library.

In this experiment we demonstrate the accuracy of the representation gener-
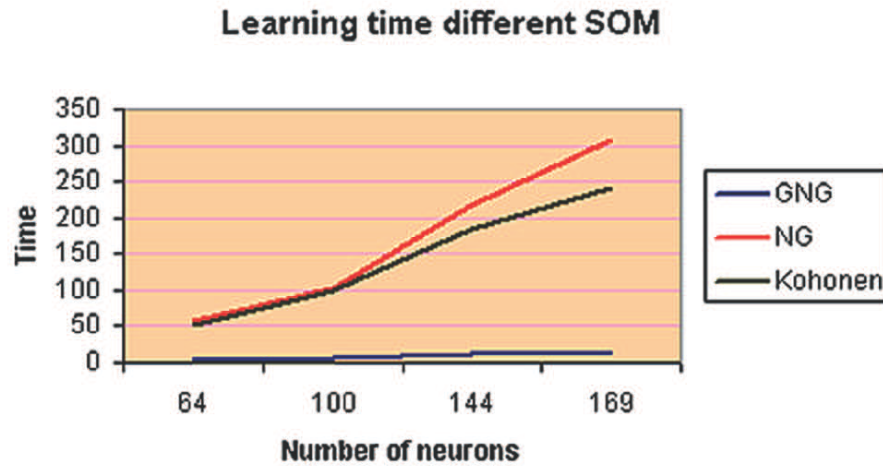
Figure 5: Learning time for various SOMs and at various neurons (in seconds).

ated by the GNG network structure compared with other filtering methods such as the Voxel Grid.

The GNG method provides a lower mean error and therefore better adaptation to the original input space, maintaining a better quality of representation in areas with a high degree of curvature and eliminating the noise generated by the sensor. The Voxel Grid method eliminates noise with the sacrifice of information loss of the input space and therefore a worse adaptation. The experiments were performed with a fixed number of points, and in the case of GNG it has been tested with different number of input signals generated by iteration, obtaining better results with a higher number of adjustments with the sacrifice of higher computation times.

In Figure 6, It can be observed how the adaption of the filtered points obtained with the Voxel Grid method produces less accurate results than the ones obtained using the GNG method. This improper adjustment for all the sections finally

generates a less accurate markers respect to the original input space. Voxel Grid method produces worse results compared to GNG method. It is shown how for a large number of sections the mean error obtained using the Voxel Grid method is higher than the one obtained using GNG.
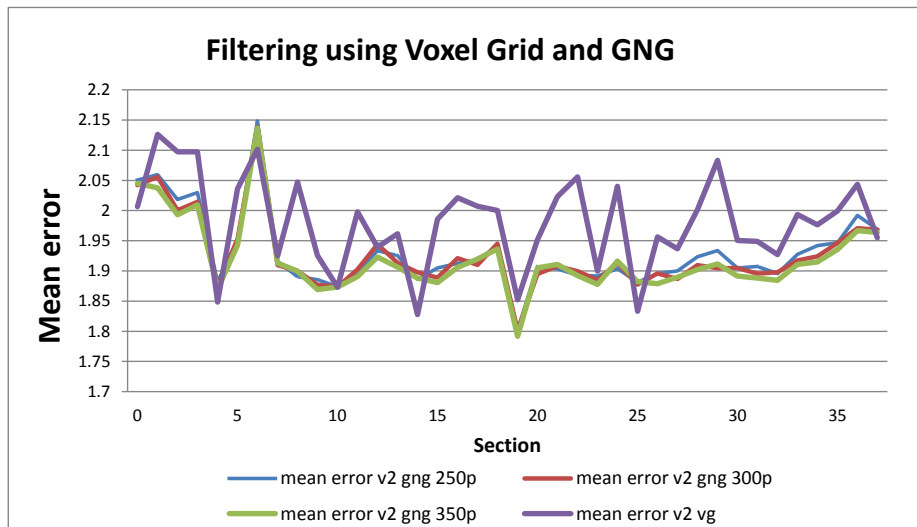

Figure 6: Voxel Grid versus GNG: Mean error for all sections (millimeters). Different number of input signals for the GNG method.

Figure 7 shows how the GNG method is more robust to noise than the Voxel Grid method. The maximum error for the ventricle slices indicate the robustness of the method for noisy inputs. The maximum error is calculated as the highest error for all the sections. The lowest maximum error is obtained using the GNG method with different number of input signals. We can visually appreciate how highest peaks of error are produced by the Voxel Grid method.

Voxel Grid method presents other drawbacks as it does not allow specifying a fixed number of points, as the number of points is given by the voxel size used for building the grid. We forced the convergence to an approximate number in our
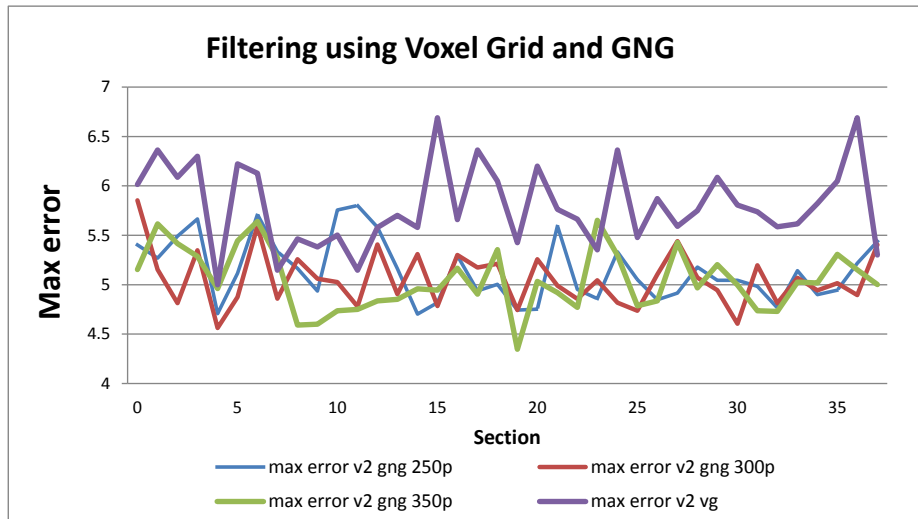
Figure 7: Voxel Grid versus GNG: Max error for all sections (millimeters). Different number of input signals for the GNG method.

experiments, making it comparison fairer. By contrast, the GNG neural network allows us to specify the exact number of end points that represent the input space.

In Figure 8 it is shown the boxplot of the mean error for all the sections. The boxplot shows that filtered sections using Voxel Grid method generates less accurate results compared to GNG (larger mean error). Moreover, the boxplot also shows how the Voxel Grid method produces more outliers and then higher errors for all the analysed sections.

4.3. 3D Reconstruction

This section shows the result of the interpolated mesh obtained by the tested methods: GNG, Poisson method, and poisson based method combined with voxelgrid [35].

In Figure 9 it is shown how Poisson surface reconstruction method, applied directly to the contours, it obtains a poor reconstruction since the method is not
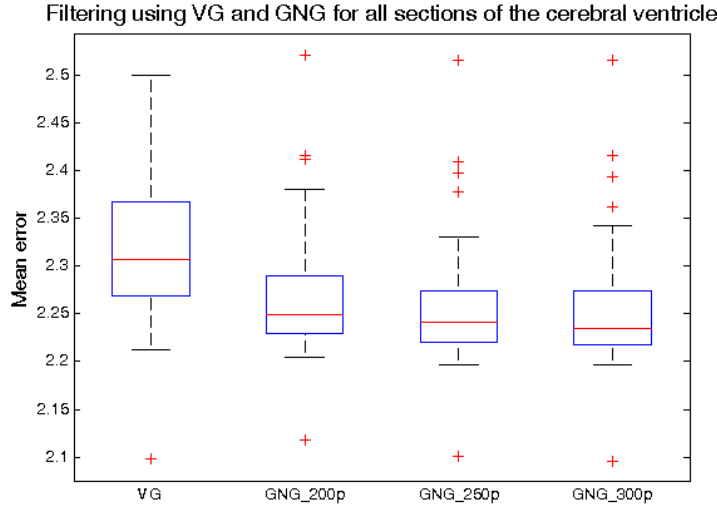
22

Figure 8: Voxel Grid versus GNG mean errors (in millimeters).

able to deal outliers and noise introduced in the acquisition process.

Figure 10 shows that using voxel grid as a preprocessing step to filter the data, poisson surface reconstruction method improves the generated representation. However, overall process is delayed as a preprocessing step (VG) has to be included. Moreover, this representation has a significant loss of accuracy in some areas which corresponds with corners and is not able to represent deformations in the ventricles that can provide doctors with evidence of some illness.

Figure 11 shows results obtained with our GNG method that combined landmarks obtained from 2D slices to build the 3D model. As can be appreciated the representation is more accurate than the one obtained with the previous method. It integrates in the same algorithm stages for: filtering, noise reduction, outlier removal and 3D reconstruction, improving the runtime of the process.
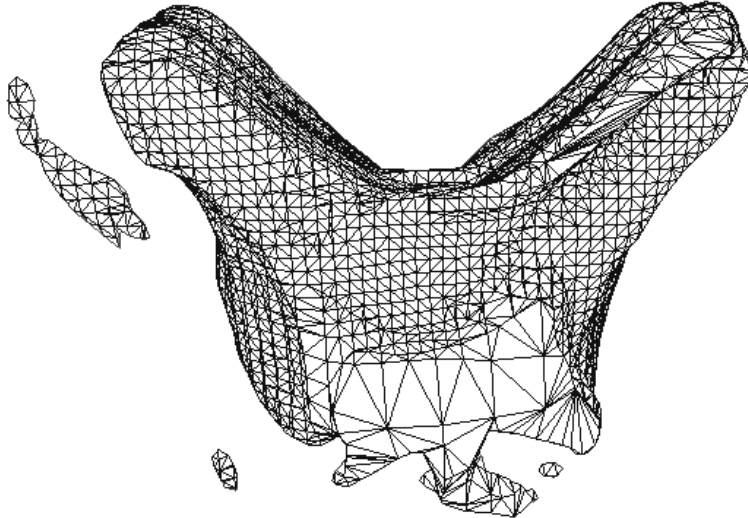
Figure 9: 3D volume generated using Poisson surface reconstruction method.

Acknowledgements

5. Conclusions

In this paper, we have used an incremental self-organising neural network (GNG) to automatically annotate landmark points on a training set of ventricle outlines. We have shown that the low dimensional incremental neural model (GNG) adapts successfully to the high dimensional manifold of the contour of the ventricles, allowing good eigenshape models to be generated completely au-
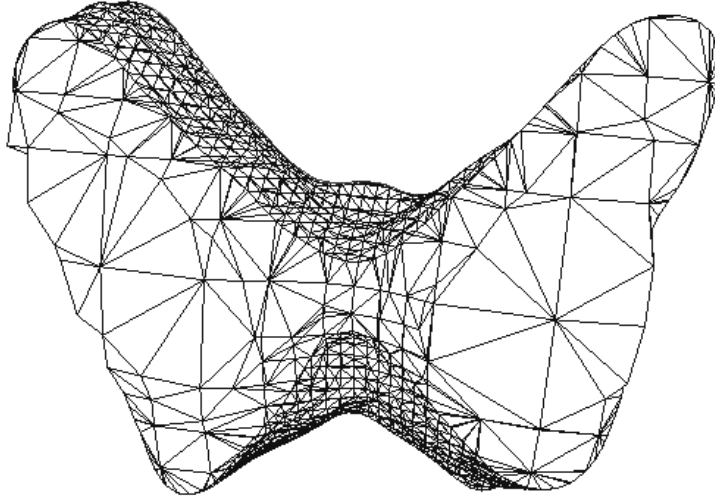
Figure 10: Poisson reconstruction combined with voxel grid downsampling.

tomatically from the training set. The accuracy of our automated segmentation algorithm is better compared to the self-organising networks NG and Kohonen both in quality and in execution time. In addition, we have shown that the optimum number of neurons required to represent the contour depends mainly on the resolution of the input space and if it is not sufficient then the topology preservation is lost or overfit. Finally, we have extended this method so that it generates $3D$ models from landmarked ventricle slices. We have compared our results with voxel grid method combined with poisson reconstruction. Our method accelerates the classical surface reconstruction and filtering processes. It is also tolerant to noise and eliminates outliers

As a further work, the generalisability of this model needs to be determined by applying it to various phantoms and other MRI standards. In addition, we will
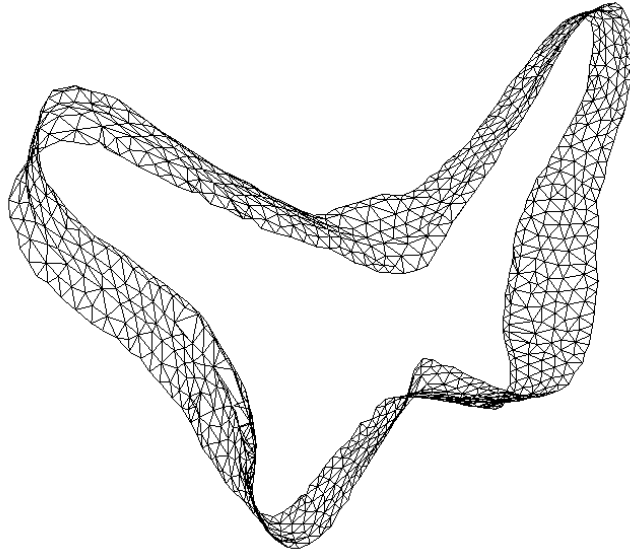
25

Figure 11: GNG 3D Volume Reconstruction.

investigate what is the most suitable number of neurons for classifying ventricles. Lastly, we will investigate applying this technology to other brain tissue components in an effort to generate a complete MRI segmentation utility.

References

[1] Nina Amenta, Sunghee Choi, and Ravi Krishna Kolluri. The power crust, unions of balls, and the medial axis transform. *Computational Geometry*, 19:127 – 153, 2001.

[2] A. Andreasen, A.M. Drewes, J.E. Assentoft, and N.E. Larsen. Computer-assisted alignment of standard serial sections without use of artificial landmarks. a practical approach to the utilization of incomplete information in 3-

d reconstruction of the hippocampal region. *Journal of Neuroscience Methods*, 45(3):199 – 207, 1992.

[3] Anastassia Angelopoulou, Alexandra Psarrou, Jose Garia-Rodriguez, and Kenneth Revett. Automatic landmarking of 2d medical shapes using the growing neural gas network. In *Proceedings of the First International Conference on Computer Vision for Biomedical Image Applications*, CVBIA'05, pages 210–219, Berlin, Heidelberg, 2005. Springer-Verlag.

[4] C. Baillard, P. Hellier, and P. Barillot. Segmentation of 3D brain structures using level sets and dense registration. *IEEE Workshop on mathematical Methods on Biomedical Image Analysis*, pages 94–101, 2000.

[5] Jean-Daniel Boissonnat. Geometric structures for three-dimensional shape representation. *ACM Trans. Graph.*, 3(4):266–286, October 1984.

[6] Lisa Gottesfeld Brown. A survey of image registration techniques. *ACM Computing Surveys*, 24:325–376, 1992.

[7] J. C. Carr, R. K. Beatson, J. B. Cherrie, T. J. Mitchell, W. R. Fright, B. C. McCallum, and T. R. Evans. Reconstruction and representation of 3d objects with radial basis functions. In *Proceedings of the 28th annual conference on Computer graphics and interactive techniques*, SIGGRAPH '01, pages 67–76, New York, NY, USA, 2001. ACM.

[8] C. Connolly. Cumulative generation of octree models from range data. In *In proceeding of: Robotics and Automation*, pages 25–32, 1984.

[9] T. F. Cootes, C. J. Taylor, D. H. Cooper, and Graham J. Training models of

shape from sets of examples. *3rd British Machine Vision Conference*, pages 9–18, 1992.

[10] Julien Dauguet, Thierry Delzescaux, Franoise Cond, Jean-Franois Mangin, Nicholas Ayache, Philippe Hantraye, and Vincent Frouin. Three-dimensional reconstruction of stained histological slices and 3d non-linear registration with in-vivo MRI for whole baboon brain. *Journal of Neuroscience Methods*, 164(1):191 – 204, 2007.

[11] H. Rhodies Davies, J. Carole Twining, F. Tim Cootes, C. John Waterton, and J. Chris Taylor. A minimum description length approach to statistical shape modeling. *IEEE Transaction on Medical Imaging*, 21(5):525–537, 2002.

[12] Tamal K. Dey and Samrat Goswami. Tight cocone: a water-tight surface reconstructor. In *Proceedings of the eighth ACM symposium on Solid modeling and applications*, SM '03, pages 127–134, New York, NY, USA, 2003. ACM.

[13] Tamal K. Dey and Samrat Goswami. Probable surface reconstruction from noisy samples. *Computational Geometry*, 35:124 – 141, 2006.

[14] Y. Ding, J.P. McAllister II, B. Yao, N. Yan, and A.I. Canady. Axonal damage associated with enlargement of ventricles during hydrocepahlus: A silver impregnation study. *Neurological Research*, 23(6):581–587, 2001.

[15] Herbert Edelsbrunner and Ernst P. Mücke. Three-dimensional alpha shapes. *ACM Trans. Graph.*, 13(1):43–72, January 1994.

[16] E. Fatemizadeh, C. Lucas, and H. Soltania-Zadeh. Automatic landmark extraction from image data using modified growing neural gas network. *IEEE Transactions on Information Technology in Biomedicine*, 7(2):77–85, 2003.

[17] Shachar Fleishman, Daniel Cohen-Or, and Cláudio T. Silva. Robust moving least-squares fitting with sharp features. *ACM Trans. Graph.*, 24(3):544–552, July 2005.

[18] B. Fritzke. A growing neural gas network learns topologies. *In Advances in Neural Information Processing Systems 7*, pages 625–632, 1995.

[19] B. Gelman, S. Dholakia, S. Casper, T.A. Kent, MW. Cloyd, and D. Freeman. Expansion of the cerebral ventricles and correlation with acquired immunodeficiency syndrome neuropathology in 232 patients. *Arch Pathol Lab Med*, 120(9):866–871, 1996.

[20] J. Geoffrey, F. Goodhill, and J. Terrence. A unifying measure for neighbourhood preservation in topographic mappings. *Proceedings of the 2nd Joint Symposium on Neural Computation*, 5:191–202, 1997.

[21] Alberto F. Goldszal, Oleh J. Tretiak, Peter J. Hand, Sanjay Bhasin, and Donald L. McEachron. Three-dimensional reconstruction of activated columns from 2-[14c]deoxy-d-glucose data. *NeuroImage*, 2(1):9 – 20, 1995.

[22] Tobias Heimann and Hans-Peter Meinzer. Statistical shape models for 3d medical image segmentation: A review. *Medical Image Analysis*, 13(4):543 – 563, 2009.

[23] Hugues Hoppe, Tony DeRose, Tom Duchamp, John McDonald, and Werner

Stuetzle. Surface reconstruction from unorganized points. *SIGGRAPH Comput. Graph.*, 26(2):71–78, July 1992.

[24] Boklye Kim, Jennifer L. Boes, Kirk A. Frey, and Charles R. Meyer. Mutual information for automated unwarping of rat brain autoradiographs. *NeuroImage*, 5(1):31 – 40, 1997.

[25] Leif Kobbelt and Mario Botsch. A survey of point-based techniques in computer graphics. *Computers & Graphics*, 28(6):801 – 814, 2004.

[26] T. Kohonen. *Self-organising maps*. Springer Verlag, 2001.

[27] Stelios Krinidis, Christophoros Nikou, and Ioannis Pitas. 3d volume reconstruction by serially acquired 2d slices using a distance transform-based global cost function. In *Proceedings of the Second Hellenic Conference on AI: Methods and Applications of Artificial Intelligence*, SETN '02, pages 390–400, London, UK, UK, 2002. Springer-Verlag.

[28] R. A. Hawkins L. S. Hibbard. Objective image alignment for three-dimensional reconstruction of digital autoradiograms. *J Neurosci Methods*, 26(1):5574., 1998.

[29] William E. Lorensen and Harvey E. Cline. Marching cubes: A high resolution 3d surface construction algorithm. *SIGGRAPH Comput. Graph.*, 21(4):163–169, August 1987.

[30] P. Markelj, D. Tomasevi, B. Likar, and F. Pernu. A review of 3d/2d registration methods for image-guided interventions. *Medical Image Analysis*, 16(3):642 – 661, 2012.

[31] T. Martinez. Competitive hebbian learning rule forms perfectly topology preserving maps. In *ICANN.*, 1993.

[32] T. Martinez, H. Ritter, and K. Schulten. Three dimensional neural net for learning visuomotor-condination of a robot arm. *IEEE Transactions on Neural Networks*, 1:131–136, 1990.

[33] T. Martinez and K. Schulten. Topology representing networks. *The Journal of Neural Networks*, 7(3):507–522, 1994.

[34] Boris Mederos, Nina Amenta, Luiz Velho, and Luiz Henrique de Figueiredo. Surface reconstruction from noisy point clouds. In *Proceedings of the Third Eurographics Symposium on Geometry Processing*, SGP '05, Aire-la-Ville, Switzerland, Switzerland, 2005. Eurographics Association.

[35] Matthew Bolitho Michael Kazhdan and Hugues Hoppe. Poisson surface reconstruction. In *Eurographics Symposium on Geometry Processing*, pages 61–70., 2006.

[36] M. Nasrabati and Y. Feng. Vector quantisation of images based upon kohonen self-organizing feature maps. In *Proc. IEEE Int. Conf. Neural Networks.*, pages 1101–1108, 1988.

[37] Sergey Osechinskiy and Frithjof Kruggel. Slice-to-volume nonrigid registration of histological sections to mr images of the human brain. *Anatomy Research International*, 2010:1–17, 2010.

[38] Sébastien Ourselin, Alexis Roche, Gérard Subsol, Xavier Pennec, and Christophe Sattonnet. Automatic Alignment of Histological Sections for 3D

Reconstruction and Analysis. Technical Report RR-3595, INRIA, December 1998.

[39] Anand Rangarajan, Haili Chui, Eric Mjolsness, Suguna Pappu, Lila Davachi, Patricia Goldman-Rakic, and James Duncan. A robust point-matching algorithm for autoradiograph alignment. *Medical Image Analysis*, 1(4):379 – 398, 1997.

[40] H. Ritter and K. Schulten. Topology conserving mappings for learning motor tasks. In *Neural Networks for Computing, AIP Conf. Proc.*, 1986.

[41] HG. Schnack, PHE. Hulshoff, WFC. Baare, MA. Viergever, and RS. Kahn. Automatic segmentation of the ventricular system from mr images of the human brain. *NeuroImage*, 14:95–104, 2001.

[42] Chen Shen, James F. O'Brien, and Jonathan R. Shewchuk. Interpolating and approximating implicit surfaces from polygon soup. *ACM Trans. Graph.*, 23(3):896–904, August 2004.

[43] A. Souza and J.K. Udupa. Automatic landmark selection for active shape models. *Proccedings of SPIE*, 2005.

[44] C. Walder, B. Schlkopf, and O. Chapelle. Implicit surface modelling with a globally regularised basis of compact support. EUROGRAPHICS, 2006.

[45] Charlie C.L. Wang. Incremental reconstruction of sharp edges on mesh surfaces. *Computer-Aided Design*, 38(6):689 – 702, 2006.

[46] S. Widz, K. Revett, and D. Slezak. An automated multi-spectral MRI seg-

mentation algorithm using approximate reducts. *Rough Sets and Current Trends in Computing*, pages 815–824, 2004.

[47] Barbara Zitov and Jan Flusser. Image registration methods: a survey. *Image and Vision Computing*, 21:977–1000, 2003.